RSC Advances

PAPER

Cite this: *RSC Adv.*, 2016, **6**, 100203

Plasmon-induced oxidative stress and macromolecular damage in pathogenic bacteria†

M. J. Silvero and M. C. Becerra*

Received 5th September 2016
Accepted 17th October 2016

DOI: 10.1039/c6ra22233a

www.rsc.org/advances

The inactivation mechanism of bacterial growth by Photodynamic Antibacterial Chemotherapy (PACT) employing gold nanoparticles and gold core/silver shell aspartame stabilized bimetallic nanoparticles was studied. Reactive oxygen species were detected and quantified, using fluorescent probes, in the first 4 h of PACT treatment on a reference strain (*Staphylococcus aureus* ATCC 29213) and two clinical isolates (an extended-spectrum β-lactamase-producing *Escherichia coli* and *Pseudomonas aeruginosa*). At the same time, damage of essential molecules such as proteins and lipids was found by spectrometric techniques and TEM images analysis. Overall, these results suggest that the oxidative stress caused by the photothermal effect of plasmon excitation leads to irreversible macromolecular damage and therefore to bacterial death. No signals of resistance to PACT with AuNP was found after a total of 31 passages of *S. aureus* treated with lower doses of the photosensitizer. All this facts support this therapy as a promising antibacterial alternative to antibiotic-resistant microbes.

Introduction

The fast rise of "superbugs" is a main challenge among current social health issues.[1–3] In depth practical research is urgently needed to deal with antibiotic-resistant bacterial strains (ARBS). It is not new that some kind of nanoparticle are very useful to eradicate bacterial infections.[4,5] Particularly, photodynamic antibacterial chemotherapy (PACT) has the potential to inactivate ARBS using nanoparticles which have special properties when their plasmon are excited;[6,7] however, it was just recently depicted that irradiated gold nanoparticles (AuNP) were able to completely inhibit the *in vivo* bacterial growth in just a few hours[8,9]. Interestingly, AuNP are chemically stable, size-controllable, easily modifiable with the desired molecules, and nontoxic to mammalian cells or animals.[10] In fact, we previously described the biocompatibility with eukaryotic cells (MTT assay).[9] As recently noted in the literature, it has been an undeniable fast progress of plasmon induced therapies in biomedicine; in contrast, their mechanism of action, pharmacokinetics, pharmacodynamics and toxicity remains poorly understood.[11] Several reports on antimicrobial photo-thermal properties of different nanoparticle could be found, but only a few studies on the process have been conducted. Often, the oxidative stress is suggested as the cause of the bacterial death without sufficient evidence.

In the present study, the mechanism of bacterial death through PACT using AuNP was deepened. The AuNP studied were synthesized by reduction of Au^{3+} with $NaBH_4$, without any further functionalization of the surface in order to investigate the AuNP's self-antibacterial activity in the dark and under irradiation at its plasmon peak at 525 nm. On the other hand, aspartame stabilized gold core/silver shell nanoparticles were also tested, given the fact that they have shown to need shorter irradiation time and less concentration compared to AuNP to achieve the bactericidal effect. A table comparing the values could be found at Fasciani *et al.* (2015).[12] Bearing in mind that plasmon excitation of AuNP could produce chemical reactions (such as a formation of radicals) in their close aqueous environment,[13] reactive oxygen species (ROS) and reactive nitrogen species (RNS) were expected to be formed in the mechanism of action. These radicals have already proved to be responsible for bacterial death caused by other nanoparticles.[14] Fluorescence Microscopy (FM) with 2′,7′-dichlorodihydrofluorescein ($DCFH_2$-DA) probe was performed for qualitative detection of this reactive species, while its quantification was carried out through fluorescence intensity measurement using 1,2,3-dihydrorhodamine (DHR). Moreover, the macromolecular damage was evaluated by measuring Advanced Oxidation Protein Products (AOPP) and oxidized lipids.[15]

The AOPP are currently used as markers of oxidative stress in plasma, due to the vulnerability of proteins to ROS and RNS. For instance, the oxidation of tyrosine (an amino-acid residue), leads to the formation of dityrosine, protein aggregation, fragmentation and crosslinking. In the presence of potassium iodide, these products can be measured spectrophotometrically at 340 nm.

Instituto Multidisciplinario de Biología Vegetal (IMBIV), CONICET and Dpto. de Farmacia, Facultad de Ciencias Químicas, Universidad Nacional de Córdoba, Ciudad Universitaria, X5000HUA Córdoba, Argentina. E-mail: becerra@fcq.unc.edu.ar

† Electronic supplementary information (ESI) available. See DOI: 10.1039/c6ra22233a

Lipid peroxidation is usually measured by the detection of its by-products: thiobarbituric acid-reactive substances.[16] This assay quantifies malondialdehyde (MDA) generated from lipid hydroperoxides. However, the disadvantage of this technique is that MDA is not a substance generated exclusively through lipid peroxidation, and besides, only certain lipid peroxidation products generate MDA. To overcome these issues, fluorescent probe carboxyfluorescein (CF) was employed. The use of liposome-entrapped CF was introduced by Weinstein *et al.* (2000) and applied by Makrigiorgos *et al.* (1997) to eukaryotic cells.[17,18] In the present work, CF was used as an indicator of membrane disruption and lipid oxidation/degradation. This method is based on the principle that CF fluoresces strongly when its concentration is reduced. Therefore, a critical amount of CF that is non-fluorescent inside the cell but fluorescent without self-quenching after release should be used. The 1 μM CF solution that was used is completely self-quenched, but the released CF levels are proportional to the loss of membrane integrity.

Transmission Electron Microscopy (TEM) images of bacteria treated with PACT using AuNP were taken to corroborate the overall structural consequence of PACT.

Results and discussion

Reactive oxygen species detection by fluorescence microscopy

Through FM, the maximum ROS levels were detected at 2 and 3 h for *S. aureus* and ESBL-producing *E. coli*, respectively, although after just 1 h, significant fluorescence was observed in the treated samples. The fluorescent intensity was remarkably higher in the treated samples, as shown in Fig. 1; however, quantitative measure was not possible through this method, though some software could make an estimate from the pictures.[19] For this reason, a different fluorescent probe DHR was used to measure ROS in the same samples.

Quantification of reactive oxygen and nitrogen species

Maximum ROS production was quantified with CF in *S. aureus*, *E. coli* and *P. aeruginosa* suspensions (10^6 CFU mL^{-1}) treated with Asp@Ag@AuNP (6.25 μM) and AuNP (2 mM). The trend was similar for the three strains, although *P. aeruginosa* (Fig. 1 – ESI†) showed higher total production of radicals in comparison to *S. aureus* and ESBL-producing *E. coli* (Fig. 2). The excited Asp@Ag@AuNP induced approximately twice the amount of ROS and RNS compare to excited AuNP and almost three times more than ciprofloxacin (CIP), even though it is known that this antibiotic is responsible for a large ROS generation, as was previously described by Becerra *et al.* (2004).[20] The slight increase in radical levels founded in the control (non-irradiated bacterial suspensions containing the core–shell nanoparticles) could be due to the effect of silver shell.[21] Nanometric silver have proved to be even more antibacterial than the bulk element, and its action it is not limited to the release of silver ions.

Detection of advanced oxidation protein products

The total increase on AOPP were similar in irradiated bacterial suspensions with AuNP and core–shell nanoparticles (around 70%), but the Asp@Ag@AuNP needed less time to induce protein damage. Fig. 3 shows the maxima amount of AOPP generated by AuNP after 6 h and Asp@Ag@AuNP after 4 h. These times are similar to those reported previously for antibiotics.[22]

It is fair to mention that the battle between bacteria and ROS it is not new under the sun. In fact, microorganisms have been fighting with them since the advent of O_2 in the atmosphere and its reaction with iron (very abundant in the early reducing atmosphere), which resulted in the formation of harmful

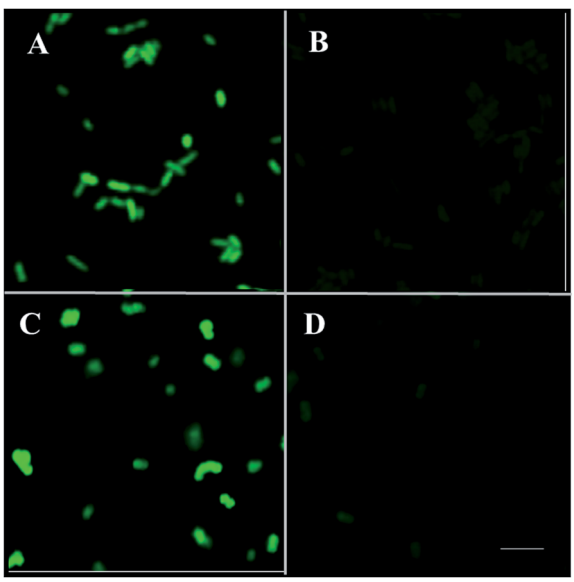

Fig. 1 FM images of (A) ESBL-producing *E. coli* treated with Asp@Ag@AuNP (B) ESBL-producing *E. coli* control without nanoparticles, (C) *S. aureus* treated with Asp@Ag@AuNP, (D) *S. aureus* control without nanoparticles, after 3 h of PACT. Scale bar is 1 μm.

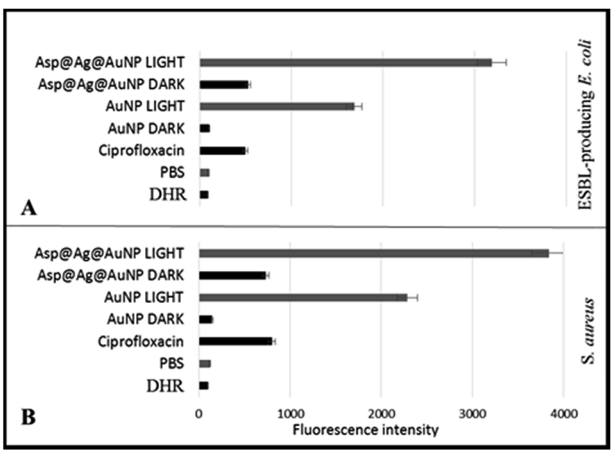

Fig. 2 ROS production after 4 h of PACT in (A) ESBL-producing *E. coli* and (B) *S. aureus* treated with Asp@Ag@AuNP (6.5 μM), AuNP (2 mM) and CIP (0.5 μg mL^{-1}). Controls without nanoparticles (PBS), without irradiation (dark) and blank of the fluorescent probe (DHR) are shown.

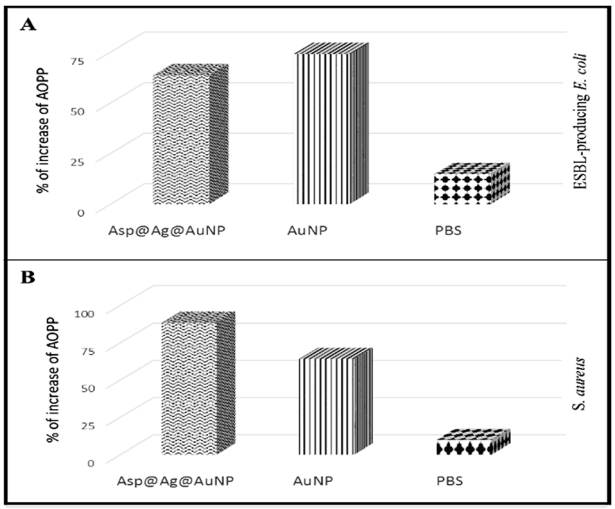

Fig. 3 Percent (%) of increase of AOPP in samples of (A) ESBL-producing *E. coli* and (B) *S. aureus* treated with PACT compare to non-irradiated ones. Control of irradiated samples without nanoparticles (PBS) are shown.

superoxide and hydroxyl radicals. This reactive species has affected all biological macromolecules (DNA, lipids and proteins), which is why living organisms had to build mechanisms to protect themselves against the oxidative stress. Although effective in normal conditions, functionality of the cell is lost when the amount of ROS produced becomes high. For this reason, novel ways to produce irreversible intracellular oxidation is still a key focus of research. In this work, two different nanomaterials demonstrate to be able to produce enough ROS to cause important protein oxidation. To the best of our knowledge, it is the first report of AOPP produced in bacteria by PACT with nanoparticles, which means the technique was adapted from the test performed in eukaryotic cells to evaluate oxidative damage.

According to previous reports, oxidized macromolecules were found in three strains (*S. aureus*, *E. coli*, and *P. aeruginosa*) treated with ceftazidime (CAZ), piperacillin, chloramphenicol, and CIP[22]. Another work describes how ROS produced by CIP in *S. aureus* could oxidize lipids. Moreover, it was found that lipid peroxidation products could interfere with superoxide dismutase (SOD), and disrupt cellular antioxidant mechanisms. This reduction in defense against oxidative stress subsequently leads to a pro-oxidant environment.[23] Furthermore, once formed, both lipid oxidized products and AOPP could cause premutagenic DNA damage with serious consequences for the cells. In this case, macromolecular damage indicator measured (AOPP) was more than twice the obtained for the untreated samples, for both an antibiotic-sensitive strain and a resistant one (Fig. 3). This suggests that defense mechanisms were sufficiently outweighed by ROS generated during PACT. These results proved the advantage of this therapy against antibiotic-resistant bacteria. There was definitively a direct relationship between the production of ROS caused by PACT with nanoparticles, the oxidation of macromolecules and the bactericidal effect, because the total growth inhibition in ESBL-producing *E. coli* and *S. aureus* was observed after 2 h of detecting the maximum AOPP amount. Clearly, antioxidant response must be activated at the very beginning of PDT treatment, which sustained the bacterial population during a few hours. However, not one of them seemed to be able to prevent major protein oxidation after large quantities of ROS were produced.

Lipid oxidation quantification

The ATCC strains exposed to AuNP presented a significant amount of oxidized lipids after only 4 h of PACT (967× and 7458× compare to non-irradiated samples) for *S. aureus* and ESBL-producing *E. coli*, respectively, while the clinical *P. aeruginosa* reached similar levels of lipid peroxidation at 8 h (6577× compare to non-irradiated samples). Results for *E. coli* could be found in Fig. 4 and data for the two other strains are available in Fig. 2 and 3 – ESI.†

The experimental results showed lipid peroxidation both in Gram negative *bacillus* (*E. coli* and *P. aeruginosa*) and in a Gram positive *coccus* (*S. aureus*). However, not all the strains had the same sensitivity to PACT. The trend found showed higher lipid peroxidation in *S. aureus*, followed by *E. coli* and *P. aeruginosa*, in that order. This result was expected because the first one is a reference strain, more sensitive to outer stress factors than the other two clinical isolates, which most likely had developed more antioxidant strategies.

Apparently, antioxidant mechanisms were overwhelmed by ROS. Indeed, other authors found that lipid peroxidation products might react and interfere with SOD, one of the key antioxidant enzymes, resulting in oxidative modifications and perturbation of cellular antioxidant mechanisms. This reduction of defenses against oxidative stress subsequently leads to a pro-oxidant condition.[24] The role of ROS in the lethal action of some antimicrobials was described in detail by Zhao *et al.* (2014).[25] Another possible cause is the fast oxidation of O_2^- to other ROS with a consequent oxidation of lipids before SOD can be effective. Once lipids are highly oxidized, serious alteration in *S. aureus* is unavoidable, as Becerra *et al.* (2006) depicted before.[26]

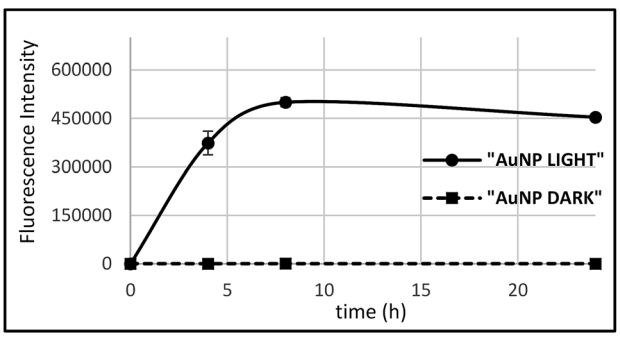

Fig. 4 Lipid oxidation on ESBL-producing *E. coli* with AuNP (2 mM) exposed to light (4 h) and kept in the dark (4 h). The fluorescence intensity of the probe CF (1 μM) is proportional to the lipid peroxidation.

TEM images of *S. aureus* with AuNP

According to TEM pictures, the AuNP were attached to the *coccus* peptidoglycan membrane. The *S. aureus* that have been in contact 4 h in the dark with AuNP still maintained their normal shape and membrane integrity (Fig. 5A–D); whereas the ones with nanoparticles that have been irradiated for 4 h showed important structural damage (Fig. 5E–H). Cui *et al.* (2012) and Zhao *et al.* (2010) found some bactericidal effect of similar gold nanoparticles *per se*, but at higher concentrations or with polymeric coating, different from the ones used in these experiments with ESBL-producing *E. coli*.[27,28] On the other hand, the membrane disruption is comparable to the one induced by cationic antibiotics such as polymyxin and gentamicin.[29,30] In addition, it is presumable that bacteria cell wall should attract positive charged AuNPs due to its total negative charge.[31] In contrast, the Asp@Ag@AuNP studied in another group's work were found inside the cell and they seemed to produce some membrane damage after just 1 h.[12] This could be explained for the silver shell bactericidal effect before irradiation,[32] which helped shorter the treatment time from 9 to 6 h. Overall, both kinds of nanoparticle showed to successfully disrupt the membrane.

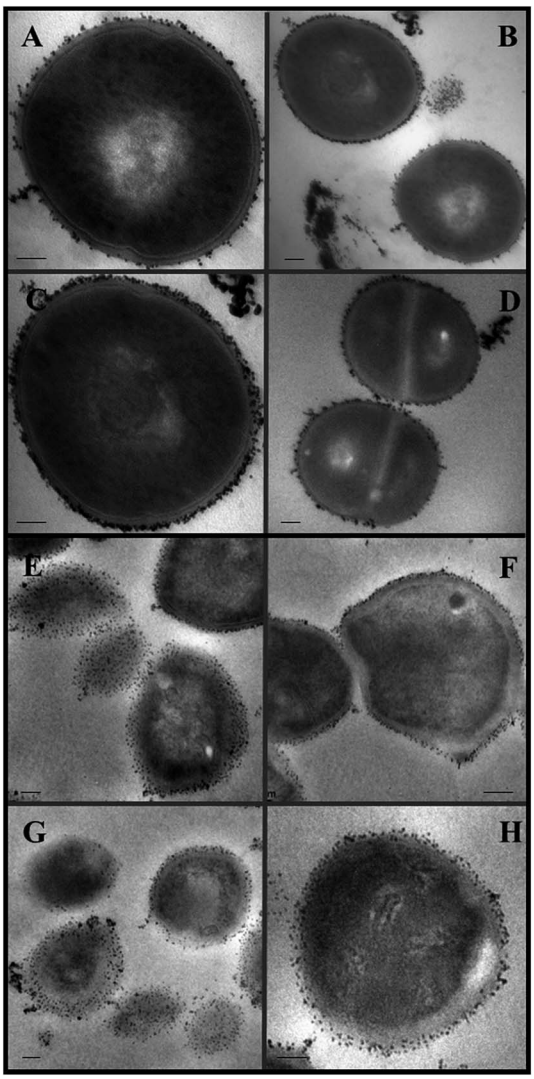

Fig. 5 Images of TEM of *S. aureus* ATCC 29213 treated with AuNP (2 mM), kept in the dark for 4 h (A–D) and exposed to light for 4 h (E–H). Scale bar is 0.1 μm.

PACT resistance development analysis

Samples of *S. aureus* treated with PACT and low concentrations of AuNP did not show any resistance to further treatment with 2 mM AuNP. By contrast, the same inoculum quickly developed resistance to CIP, acquiring 10-fold the original Minimal Inhibitory Concentration (MIC) (5 μg mL^{-1}) after just 10 passages. Neither control did display significant changes along the 31 passages. Bacteria usually evolve strategies for resistance against antibiotics after a few dozens of new generations and drugs which could avoid or delay resistance are much more suitable for clinical use.[33] We believe that the strong photothermal effect of PACT with AuNP and the large amount of ROS generated make it difficult for bacteria to employ existing strategies for resistance compared to small molecule antibiotics.[34]

Experimental section

Bacterial strains and controls

The experiments were performed testing *S. aureus* ATCC 29213, *S. aureus* ATCC 25923, an extended-spectrum beta-lactamase-producing (ESBL) *E. coli* and *P. aeruginosa*; these last two were clinical strains provided by the Bacteriology Service of Sanatorio Aconcagua from Córdoba, Argentina. Stock cultures were maintained in trypticase soy broth and stored frozen in 10% glycerol. Ciprofloxacin (CIP), a commercial antibiotic, was always used as a positive control for bactericidal effect and oxidative stress.[35,36]

Synthesis of AuNP and Asp@Ag@AuNP

AuNP and Asp@Ag@AuNP used in this work were synthesized as in previous works with Scaiano's group.[9,12] Spectra of colloidal AuNP were recorder employing an Agilent 8243 spectrophotometer with DAD detector, using a cell with an optical path length of 1 cm, to select same size, shape and concentration for all batches.

Reactive oxygen species detection by fluorescence microscopy

As a first approach, ROS production was detected qualitatively by FM (Axiovert 135M-Carl Zeiss). A drop of bacterial suspension (10^9 CFU mL^{-1} of *S. aureus* and ESBL-producing *E. coli*) treated with Asp@Ag@AuNP (6.25 μM) and AuNP (2 mM) and irradiated at 525 nm for 1, 2, 3 and 4 h was placed on a microscope glass without any fixation procedure. In order to observe the ROS production through the FM in the fresh sample, the fluorescent probe $DCFH_2$-DA (1 μM) was added immediately. CIP (0.5 μg mL^{-1}) was used as a positive control. Proper non-irradiated and not-treated controls were run. All the samples were analyzed in triplicates, and the experiment was reproduced in two different weeks.

Quantification of reactive oxygen and nitrogen species

The pre-fluorescent probe DHR was chosen for its high sensitivity to quantify total ROS and RNS.[37] This dye diffuses passively through most of cell membranes, where cationic (DHR) generates a fluorescent green signal at 536 nm when oxidized. Radical indicators of oxidative stress were measured with DHR (1 μM) in bacterial suspensions (10^9 CFU mL^{-1}) treated with a 1 : 1 ratio with Asp@Ag@AuNP (6.25 μM) and AuNP (2 mM). Samples were incubated for 2, 4 and 6 h at 37 °C (in darkness and under irradiation at 525 nm). CIP (0.5 μg mL^{-1}) was used as a positive control.

Detection of advanced oxidation protein products

In order to evaluate protein oxidation after PACT, the AOPP generation using Asp@Ag@AuNP (6.25 μM) and AuNP (2 mM) was studied on bacterial suspensions. These oxidized products, in the presence of potassium iodide were measured spectrophotometrically at 340 nm. The measurements were performed after 1, 2, 4, 6 and 8 h. The calibration curve was performed using chloramine T and total proteins were detected with Bradford reagent. Once more, CIP (0.5 μg mL^{-1}) was used as a positive control. The results were expressed as a percentage (%) of increase in the irradiated samples AOPP (4 h) compare to the ones kept in the dark.[24]

Lipid oxidation quantification

Lipid oxidation was quantified kinetically during 24 h of irradiation in the same samples mentioned above using the highly sensitive fluorescent probe CF (1 μM). All the conditions were tested in triplicate and SD calculated was never above 5%.[16]

TEM images of *S. aureus* with AuNP

Suspensions of *S. aureus* ATCC 29213 (10^9 CFU mL^{-1}) in phosphate saline buffer (PBS) were incubated with aqueous AuNPs (2 mM) in a 50 : 50 ratio for 4 h. One wellplate was irradiated with a 525 nm LED panel (Fig. 3 – ESI†) and the other one was kept in the dark. Well content was then collected and centrifuged for 15 min at 1000 rpm. The pellets were washed four times and finally fixed in 2% glutaraldehyde and 4% formaldehyde solutions in 0.1 M cacodylate buffer for 2 h at room temperature, and then post-fixed with osmium tetroxide at 1% in the same buffer, dehydrated and embedded in Araldite. Thin sections were cut with a diamond knife on a JEOL JUM-7 ultramicrotome, mounted on nickel grids and examined in a Zeiss LEO 906E electron microscope. The quality of the pictures was optimized to analyze in detail the nanoparticles localization, the cell shape and membrane state by an improved sample preparation.[9] Cropping on pictures was performed. Original brightness and contrast were not modified. Selected images are representative of the total bacteria population.

PACT resistance development analysis

The development of resistance was tested in a total of 31 sustained passages of *S. aureus* ATCC 25923. Briefly, an inoculum of 10^6 was incubated in a 50 : 50 ratio with 6.66 mM (2/3 of 2.00 mM, the concentration needed to achieve complete photoinhibition) in M9 medium at 37 °C for 18 h under irradiation (525 nm).[33] After each passage, the sample was treated with PACT using 2 mM AuNP and CFU mL^{-1} counting was performed after additional 18 h. Non-irradiated, nanoparticles-free and antibiotic-treated *S. aureus* suspensions were cultured as well as a control in every passage. The antibiotic used was CIP at 2/3 of its MIC (0.16 μM).

Conclusion

This study focused mainly on understanding the effect of nanophotosensitizers on the structure and physiology of prokaryotic cell treated with PACT. Presumed ROS and RNS production and their effect on bacterial proteins and lipids were confirmed. These results support the proposed mechanism for PACT with AuNP. According to this experimental data, bacterial death is caused as the result of macromolecular damage by large amounts of radicals produced after plasmon excitation of AuNP (attached to the membrane) and excitation of the gold core of bimetallic nanoparticles (located inside the cell). Additionally, the silver on core–shell nanoparticles have probed to increase the oxidative stress, reducing the PACT treatment time. Moreover, PACT treated bacteria did not show any development of resistance; this would be a major advantage to small molecules antibiotics. We hope these findings will stimulate further research on the field.

Author contributions

MJS and MCB planned the assays and analyzed the results. MJS conducted all the experiments and write the manuscript under MCB supervision.

Conflict of interest

The authors declare no competing financial interest.

Funding sources

This work was supported by Secretaría de Ciencia y Tecnología de la Universidad Nacional de Córdoba (SECyT-UNC), Fondo para la Investigación Científica y Tecnológica (FONCyT): Préstamo BID Proyecto de Investigación en Ciencia y Tecnología (PICT 2014) grant no. 821, and Consejo Nacional de Investigaciones Científicas y Técnicas (CONICET), Proyecto de Investigación Plurianual (PIP 2012–2014) grant no. 11220110100965.

Acknowledgements

We would like to thank Tito Scaiano for his key advices on the revised manuscript; Dr Pilar Crespo from CIBICI-CONICET and Dr Cristina Maldonado from the Centro de Biología Molecular – Universidad Nacional de Córdoba for their support on microscopy imaging, as well as Pharmacist Sol Martinez for her assistance with experimental protocols, Biochemist Andrea Piersigilli for providing the clinical strains, Engineer Álvaro

E. Garbiglia for the design and construction of the LED panel and Gil Michell, language translator, for the manuscript revision.

References

1 R. Smith, *Bull. W. H. O.*, 1999, **77**, 862.
2 J. Coast, R. Smith and M. Miller, *Health Econ.*, 1996, **5**, 217–226.
3 *Bulletin of the World Health Organization*, Print version ISSN 0042-9686, Genebra, 2002, vol. 80, suppl. 2.
4 Y. Luo, M. Hossain, C. Wang, Y. Qiao, J. An, L. Ma and M. Su, *Nanoscale*, 2013, **5**, 687–694.
5 S. Yash, R. R. Stone, B. Fellows, B. Qi, G. Huang, O. Thompson Mefford and T.-R. J. Tzeng, *Nanoscale*, 2015, **7**, 8326–8331.
6 W. Q. Lim and G. Zhiqiang, *Nano Today*, 2016, **11**, 168–188.
7 P. C. Ray, S. A. Khan, A. K. Singh, D. Senapati and Z. Fan, *Chem. Soc. Rev.*, 2012, **41**, 3193–3209.
8 X. Li, M. Robinson, A. Gupta, K. Saha, Z. Jiang, D. F. Moyano, A. Sahar, M. A. Riley and V. M. Rotello, *ACS Nano*, 2014, **8**, 10682–10686.
9 M. J. Silvero, G. A. Argüello and M. C. Becerra, *Journal of Nanopharmaceutics and Drug Delivery*, 2014, **2**, 1–5.
10 N. L. Rosi, D. A. Giljohann, C. S. Thaxton, A. K. Lytton-Jean, M. S. Han and C. A. Mirkin, *Science*, 2006, **312**, 1027–1030.
11 W. Qi Lim and Z. Gao, Plasmonic nanoparticles in biomedicine, *Nano Today*, 2016, **11**(2), 168–188.
12 C. Fasciani, M. J. Silvero, M. A. Anghel, G. A. Arguello, M. C. Becerra and J. C. Scaiano, *J. Am. Chem. Soc.*, 2014, **136**(50), 17394–17397.
13 C. G. Silva, R. Juárez, T. Marino, R. Molinari and H. J. García, *J. Am. Chem. Soc.*, 2011, **133**(3), 595–602.
14 J. Li, H. Zhou, J. Wang, D. Wang, R. Shen, X. Zhang, P. Jin and X. Liu, *Nanoscale*, 2016, **8**, 11907–11923.
15 E. Cabiscol, J. Tamarit and J. Ros, *Int. Microbiol.*, 2000, **3**, 3–8.
16 B. Halliwell and S. Chirico, *Am. J. Clin. Nutr.*, 1993, **57**(5), 715S–724S.
17 E. A. Weinstein, H. Li, J. A. Lawson, J. Rokach, G. A. FitzGerald and P. H. Axelsen, *J. Biol. Chem.*, 2000, **275**, 22925–22930.
18 G. M. Makrigiorgos, A. L. Kassis, A. Mahmood, F. A. Bump and P. Savvides, *Free Radical Biol. Med.*, 1997, **22**, 93–100.
19 J. Selinummi, J. Seppälä, O. Yli-Harja and J. A. Puhakka, *BioTechniques*, 2005, **39**, 859–863.
20 M. C. Becerra, M. Sarmiento, P. L. Páez, G. A. Argüello and I. Albesa, *J. Photochem. Photobiol., B*, 2004, **76**, 13–18.
21 S. Mukherjee, D. Chowdhury, R. Kotcherlakota, S. Patra, B. Vinothkumar, M. P. Bhadra, B. Sreedhar and C. R. Patra, *Theranostics*, 2014, **4**, 3.
22 P. L. Páez, M. C. Becerra and I. Albesa, *Cell Biochem. Biophys.*, 2011, **61**(3), 467–472.
23 B. Uttara, A. V. Singh, P. Zamboni and R. T. Mahajan, *Curr. Neuropharmacol.*, 2009, **7**(1), 65–74.
24 M. H. Lee and J. W. Park, *Biochem. Mol. Biol. Int.*, 1995, **35**(5), 1093–1102.
25 X. Zhao and K. Drlica, *Curr. Opin. Microbiol.*, 2014, **21**, 1–6.
26 M. C. Becerra, P. L. Páez, L. E. Laróvere and I. Albesa, *Mol. Cell. Biochem.*, 2006, **285**, 29–34.
27 Y. Cui, Y. Zhao, Y. Tian, W. Zhang, X. Lü and X. Jiang, *Biomaterials*, 2012, **33**(7), 2327–2333.
28 Y. Zhao, Y. Tian, Y. Cui, W. Liu, W. Ma and X. Jiang, *J. Am. Chem. Soc.*, 2010, **132**(35), 12349–12356.
29 M. Vaara and T. Vaara, *Antimicrob. Agents Chemother.*, 1983, **24**, 114–122.
30 J. L. Kadurugamuwa, A. J. Clarke and T. J. Beveridge, *J. Bacteriol.*, 1993, **175**, 5798–5805.
31 J. C. Scaiano, P. Billone, C. Gonzalez, L. Maretti, M. L. Marin, K. L. McGilvray and N. Yuan, *Pure Appl. Chem.*, 2009, **81**(4), 635–647.
32 Y. Zhou, Y. Kong, S. Kundu, J. D. Cirillo and H. Liang, *J. Nanobiotechnol.*, 2012, 10–19.
33 S. B. Levy and B. Marshall, *Nat. Med.*, 2004, **10**(12), S122–S129.
34 I. Chopra, *J. Antimicrob. Chemother.*, 2007, **59**(4), 587–590.
35 M. C. Becerra and I. Albesa, *Biochem. Biophys. Res. Commun.*, 2002, **297**(4), 1003–1007.
36 M. C. Becerra, A. J. Eraso and I. Albesa, *Luminescence*, 2003, **18**(6), 334–340.
37 S. I. Dikalov and D. G. Harrison, *Antioxid. Redox Signaling*, 2014, **20**(2), 372–382.